

# Icariside II inhibits cell proliferation and induces cell cycle arrest through the ROS-p38-p53 signaling pathway in A375 human melanoma cells

JINFENG WU<sup>1\*</sup>, TAO SONG<sup>2\*</sup>, SHUYONG LIU<sup>3</sup>, XIAOMEI LI<sup>4</sup>, GANG LI<sup>1</sup> and JINHUA XU<sup>1</sup>

<sup>1</sup>Department of Dermatology, Huashan Hospital, Fudan University, Shanghai, 200040; <sup>2</sup>Department of Neurosurgery, Provincial Hospital Affiliated to Shandong University, Jinan, Shandong 250021; <sup>3</sup>Department of Radiology, Tai'an City Central Hospital, Tai'an, Shandong 271000; <sup>4</sup>Cancer Center, The Second Hospital of Shandong University, Jinan, Shandong 250033, P.R. China

Received August 6, 2013; Accepted July 23, 2014

DOI: 10.3892/mmr.2014.2701

**Abstract.** Icariside II (IS) is a metabolite of icariin, which is derived from *Herba Epimedii*. In the present study, the antiproliferative effects of IS on A375 human melanoma cells were examined *in vitro* and a possible mechanism through the ROS-p38-p53 pathway is discussed. A cell WST-8 assay revealed that treatment with IS markedly reduced cell viability from 77 to 21% (25 and 100  $\mu$ M, respectively), and cell counting demonstrated that IS treatment reduced cell proliferation. IS treatment also induced cell cycle arrest of A375 cells at the G0/G1 and G2/M transitions and inhibited the expression of cell-cycle related proteins, including cyclin E, cyclin-dependent kinase 2 (CDK2), cyclin B1 and phosphorylated cyclin-dependent kinase 1 (P-CDK1). In this study, it was determined that IS inhibits cell proliferation and induces cell cycle arrest through the generation of reactive oxygen species and activation of p38 and p53. These findings were further supported by the evidence that pretreatment with *N*-acetyl-L-cysteine, SB203580 or pifithrin- $\alpha$  significantly blocked IS-induced reduction of cell viability, increase of cell death and cell cycle arrest. In conclusion, IS inhibits cell proliferation and induces cell cycle arrest. Crucially, it was confirmed that these effects were mediated at least in part by activating the ROS-p38-p53 pathway.

## Introduction

Melanoma is the fifth most frequently diagnosed type of malignancy in males and the sixth in females in the USA (1).

Furthermore, its high rate of invasiveness and dissemination makes surgery an unlikely option, with the exception of rare cases (2). Despite the development of new modalities of therapy, the outcome for patients with advanced melanoma is extremely poor (3). Current standard treatment includes the single-agent dacarbazine which improves clinical response but not the median survival duration (4,5).

Future improvements in melanoma treatment are likely to arise from novel agents which target molecular pathways that regulate tumor cell growth and survival. In accordance with present research development, the mitogen-activated protein kinases (MAPKs) pathway is an attractive target for therapeutic intervention in melanoma (6). MAPKs have an important role in the regulation of numerous cellular processes, including cell growth and proliferation, differentiation, and apoptosis. MAPKs consist of extracellular signal-related kinases (ERKs), c-Jun NH<sub>2</sub>-terminal kinases (JNKs) and p38 MAPKs (7). Previous studies have indicated that the activation of p38 MAPK is involved in cell growth arrest and apoptosis via the generation of reactive oxygen species (ROS) (8,9). It has also been reported that p38 activation leads to accumulation of p53, a major tumor suppressor protein (10). p53-dependent cell cycle arrest is mainly mediated by transcriptional activation of p21 (11).

Previous studies indicate that ROS generation, by which a number of anti-cancer agents act, is in part responsible for the cytotoxic efficacy in a numerous types of tumor cell (12,13). Icariside II (IS) is a metabolite of icariin, which is derived from *Herba Epimedii*. IS is a novel anticancer drug that induces apoptosis in tumor cell lines (14-16). In the present study, the antiproliferative effects of IS on A375 human melanoma cells *in vitro* are evaluated and the possible mechanism through the ROS-p38-p53 signaling pathway is demonstrated.

## Materials and methods

**Reagents and cell culture.** Icariside II (>98% pure) (Fig. 1A) was isolated by the enzymatic hydrolysis of icariin (Shanghai Ronghe Pharmaceutical Company, Shanghai, China), as previously described (17). The A375 human melanoma cells were purchased from American Type Culture Collection (Manassas,

---

*Correspondence to:* Dr Jinhua Xu or Dr Gang Li, Department of Dermatology, Huashan Hospital, Fudan University, 12 Middle Urumqi Road, Shanghai 200040, P.R. China  
E-mail: jhXu2012@gmail.com  
E-mail: ganglihs@163.com

\*Contributed equally

**Key words:** icariside II, melanoma, cell proliferation, reactive oxygen species, p38, p53

VA, USA) and maintained in Dulbecco's modified Eagle's medium (DMEM; Invitrogen, Carlsbad, CA, USA) containing 4 mM L-glutamine, 3.7 g/l sodium bicarbonate, 4.5 g/l glucose and 10% fetal bovine serum (FBS; Invitrogen). Cells were maintained in a 5% CO<sub>2</sub> humidified incubator at 37°C. WST-8 was obtained from Dojindo (Mashikimachi, Japan), propidium iodide (PI) and RNaseA were supplied by Beyotime Institute of Biotechnology (Haimen, China). Rabbit monoclonal (P)-p38, mouse monoclonal P-p53, mouse monoclonal p21, rabbit polyclonal P-cyclin-dependent kinase 1 (P-CDK1), rabbit monoclonal cyclin-dependent kinase 2 (CDK2), mouse polyclonal cyclin E, rabbit monoclonal cyclin B1, rabbit monoclonal cleaved poly (ADP-ribose) polymerase (PARP) and mouse monoclonal  $\beta$ -actin antibodies were obtained from Cell Signaling Technology, Inc. (Beverly, MA, USA). N-acetyl-L-cysteine (NAC), SB203580 and pifithrin- $\alpha$  were supplied by Sigma-Aldrich (St. Louis, MO, USA). Horse radish peroxidase-conjugated secondary anti-mouse IgG and anti-rabbit IgG antibodies were provided by Cell Signaling Technology, Inc.

**Cell viability assays.** IS dissolved in dimethylsulfoxide (DMSO) was used for the treatment of cells. The final concentration of DMSO used was <0.1% (v/v). Cell viability was measured using the WST-8 assay from Dojindo following the optimized manufacturer's instructions. The A375 cells were seeded at a density of 3,000 cells/well in 96-well culture plates in DMEM and incubated in a humidified incubator at 37°C overnight. The cells were pretreated with or without NAC (2 mM), SB203580 (5  $\mu$ M), or pifithrin- $\alpha$  (5  $\mu$ M) for 1 h. Then the cells were treated with different concentrations of IS (0, 25, 50 or 100  $\mu$ M). After 24 h of post-treatment incubation, 10  $\mu$ l WST-8 was added to each well for 1 h. Subsequently the optical density (OD) was measured at 450 nm. The percentage of viable cells was determined by the following formula: Ratio = [(OD<sub>IS</sub>-OD<sub>blank</sub>)/(OD<sub>control</sub>-OD<sub>blank</sub>)] x 100. The cell viability data are averages of three independent experiments each containing six replicates.

**Cell proliferation assays.** The A375 cells were seeded at a density of 2x10<sup>5</sup> cells/well in 6-well culture plates in DMEM and incubated in a humidified incubator at 37°C for 24 h prior to treatment with different concentrations of IS (0, 25, 50 or 100  $\mu$ M). After 24 h of post-treatment incubation, the cells were harvested and resuspended in 1 ml DMEM. Following resuspension, 100  $\mu$ l cells were added to a CASY cup containing 10 ml CASY ton (Roche, Mannheim, Germany), an electrolyte/buffer. The detection of living and total cell numbers was determined by the Casy Cell Counter and Analyzer system (Roche) (18,19).

**Cell cycle and cell death analysis.** For cell cycle analysis, A375 cells were seeded at a density of 2x10<sup>5</sup> cells/well in 6-well culture plates in DMEM and incubated in a humidified incubator at 37°C for 24 h. Then the cells were starved with fetal bovine serum-free DMEM for 24 h. Subsequently, the cells were pretreated with or without NAC (2 mM), SB203580 (5  $\mu$ M) or pifithrin- $\alpha$  (5  $\mu$ M) for 1 h. Next the cells were treated with different concentrations of IS (0, 25, 50 or 100  $\mu$ M) for 24 h. Following incubation, cells were collected and fixed in 70% ethanol for 24 h at 4°C. The cells were centrifuged at 245 x g for 5 min and the cell pellet

was resuspended in 400  $\mu$ l phosphate-buffered saline (PBS) containing RNase A (10 mg/ml, 50  $\mu$ l) and PI (2 mg/ml, 10  $\mu$ l). The mixture was incubated in the dark at 37°C for 30 min and then analyzed using a FACSCalibur™ cytometer (BD Biosciences, San Jose, CA, USA). The cell cycle and cell death data were analyzed using FlowJo software V6.0 (Tree star, Ashland, OR, USA). The relative DNA content per cell was obtained by measuring the fluorescence of the DNA. The extent of cell death was determined by evaluating the sub G1 fraction, or the percentage of cells with DNA content <2N. The data were replicated three times.

**Western blot assays.** A375 cells were pretreated with or without NAC (2 mM), SB203580 (5  $\mu$ M) or pifithrin- $\alpha$  (5  $\mu$ M) for 1 h. This was followed by treatment with different concentrations of IS (0, 25, 50 and 100  $\mu$ M) for 24 h. The cells were resuspended in lysis buffer (150 mmol/l NaCl, 1% NP-40, 0.5% sodium deoxycholate, 0.1% SDS, and 50 mmol/l Tris-Cl pH 8.0, 2  $\mu$ g/ml aprotinin, 2  $\mu$ g/ml leupeptin, 40 mg/ml of phenylmethylsulfonyl fluoride, 2 mmol/l dithiothreitol; Beyotime Institute of Biotechnology) and centrifuged at 10,080 x g for 15 min to remove nuclei and cell debris. Supernatants were frozen at -80°C until use. The protein concentrations were determined by the Bradford assay (Bio-Rad, Hercules, CA, USA) and 30  $\mu$ g cellular proteins were electroblotted onto a polyvinylidene fluoride membrane (Millipore, Billerica, MA, USA) following separation using 10% SDS-polyacrylamide gel electrophoresis. The immunoblot was blocked for 1 h with 5% milk at room temperature followed by an overnight incubation at 4°C with a 1:1,000 dilution of primary antibodies against P-p38, P-p53, p21, P-CDK1, CDK2, cyclin E, cyclin B1, cleaved PARP or  $\beta$ -actin. Blots were washed twice with Tween 20/Tris-buffered saline (TTBS) prior to addition of a 1:1,000 dilution of horseradish peroxidase-conjugated secondary antibody for 1 h at room temperature. Blots were again washed with TTBS [Sangon Biotech (Shanghai) Co., Ltd., Shanghai, China] before development by enhanced chemiluminescence using Supersignal West Femto Chemiluminescent substrate (Pierce, Rockford, IL, USA). Band intensities were quantified using UN-SCAN-IT Gel Analysis software (version 6; Silk Scientific, Orem, UT, USA). The optical density for the target protein was shown as a proportion of the  $\beta$ -actin optical density. The western blot data were replicated three times.

**Evaluation of ROS.** ROS were detected using the cell-permeable fluorescent probe 2,7-dichlorodihydrofluorescein diacetate (H<sub>2</sub>DCFDA; Sigma-Aldrich), a non-fluorescent compound, which is converted into highly fluorescent dichlorodihydrofluorescein by cellular peroxides. The A375 cells were exposed to various concentrations of IS (0, 25, 50 and 100  $\mu$ M) for 6 h and were then loaded with H<sub>2</sub>DCFDA (10  $\mu$ M) in serum-free DMEM. Following incubation at 37°C for 30 min, cells were washed with PBS and fluorescence was monitored by flow cytometry at excitation wavelength of 488 nm and an emission wavelength of 530 nm. The mean fluorescence intensity (MFI) data was analyzed using FlowJo software V6.0. The MFI data were replicated three times.

**Statistics.** All data are presented as the mean  $\pm$  standard deviation. Data analysis was performed by one-way analysis

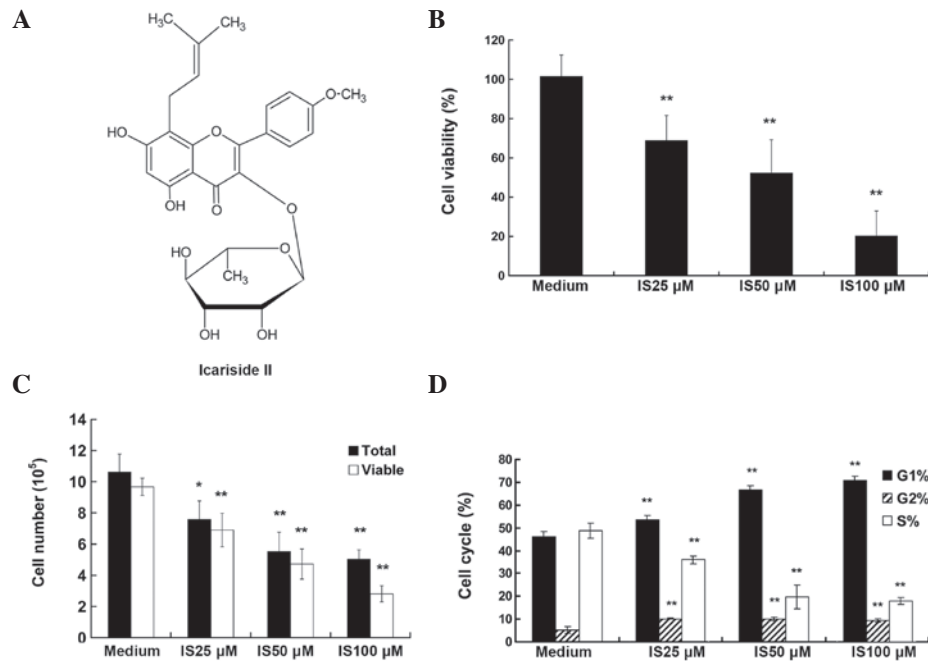


Figure 1. Icariside II (IS) inhibits cell viability and proliferation and induces cell cycle arrest in A375 cells. (A) Chemical structure of IS. (B) Cell viability of A375 cells as measured by the WST-8 assay. Cells were treated with IS at various concentrations (0, 25, 50 and 100  $\mu$ M) for 24 h prior to the addition of WST-8 for 1 h. Then the optical density data were detected in a plate reader at 450 nm. (C) Cell proliferation assays. A375 cells were seeded at a density of  $2 \times 10^5$  cells/well and treated with different concentrations of IS (0, 25, 50 and 100  $\mu$ M) for 24 h. The detection of living and total cell numbers was determined by the Casy Cell Counter and Analyzer system. (D) Cell cycle analysis. A375 cells were starved with fetal bovine serum-free medium for 24 h. The cells were then treated with different concentrations of IS (0, 25, 50 and 100  $\mu$ M) for 24 h. After fixation, the cells was stained with propidium iodide and then analyzed using a FACSCalibur™ cytometer. The data were analyzed using FlowJo software V6.0. The cell cycle data were replicated three times. \*\*P<0.01, as compared with medium control.

of variance. For comparison of two groups, a Student's t-test was used. P<0.05 was considered to indicate a statistically significant difference.

## Results

**IS inhibits cell viability and proliferation in A375 cells.** The viability of A375 cells was tested following treatment with increasing concentrations of IS (0, 25, 50 and 100  $\mu$ M) for 24 h. As demonstrated by the WST-8 assay, treatment with IS resulted in markedly reduced cell viability, from 77 to 21% (25 and 100  $\mu$ M respectively; P<0.01) (Fig. 1B). The detection of living and total cell numbers was determined by the Casy Cell Counter and Analyzer system. As displayed in Fig. 1C, following a 24-h incubation period, the total cell numbers in the medium control group was increased from  $2.00 \times 10^5$  to  $10.62 \times 10^5$ , and IS treatment significantly decreased total cell numbers, as compared with that of the medium control group (P<0.01). For example, only  $5 \times 10^5$  total cells were counted in the IS 100  $\mu$ M treatment group. A similar trend was observed in the living cells data (P<0.01).

**IS induces cell cycle arrest and inhibits the expression of cell cycle-related proteins in A375 cells.** As a reduction in cell proliferation may result from the induction of cell cycle arrest, the present study investigated whether the IS-induced growth inhibition was due to cell cycle arrest. Cell cycle distribution analysis (Fig. 1D) showed that the percentage of cells in G0/G1 phase increased with the increasing IS concentration and peaked at 100  $\mu$ M of IS (69.51%), as compared with that of the medium

control group (44.01%). By contrast, the percentage of cells in the S phase was reduced accordingly (P<0.01). Additionally, IS treatment induced G2/M arrest (P<0.01), although to a lesser extent. The cell cycle is regulated by cyclins and cyclin-dependent kinases (20). As demonstrated by western blot assay (Fig. 2), 50 and 100  $\mu$ M IS treatment significantly inhibited the expression levels of cyclin E, CDK2, cyclin B1 and P-CDK1 (P<0.01), while 25  $\mu$ M IS treatment only caused a significant reduction in the expression levels of cyclin E (P<0.01).

**IS induces the production of ROS and activates p38, p53 and p21.** To investigate the molecular mechanism for IS-induced cell cycle arrest, the present study examined whether IS induces the generation of ROS. The levels of ROS were determined 6 h after IS treatment. As shown in Fig. 3A and B, flow cytometry revealed that IS-induced ROS generation was ~2.3-fold higher compared with that in the medium controls (25  $\mu$ M; P<0.01). A previous study has shown that ROS induce cell cycle arrest via activation of p38, p53 and p21 (20). In the present study, western blot analysis demonstrated that IS (25, 50 and 100  $\mu$ M) treatment significantly increased the phosphorylation of p38 and p53 compared with that in the medium controls (P<0.01; Fig. 3C and D). An increased expression level of p21 was also observed following IS treatment compared with that in the medium controls (P<0.01).

**NAC, SB203580, and pifithrin-a reverse the effects of IS on cell viability, cell cycle arrest and cell death.** As demonstrated by WST-8 assay (Fig. 4A), treatment with 50  $\mu$ M IS for 24 h significantly reduced cell viability compared with

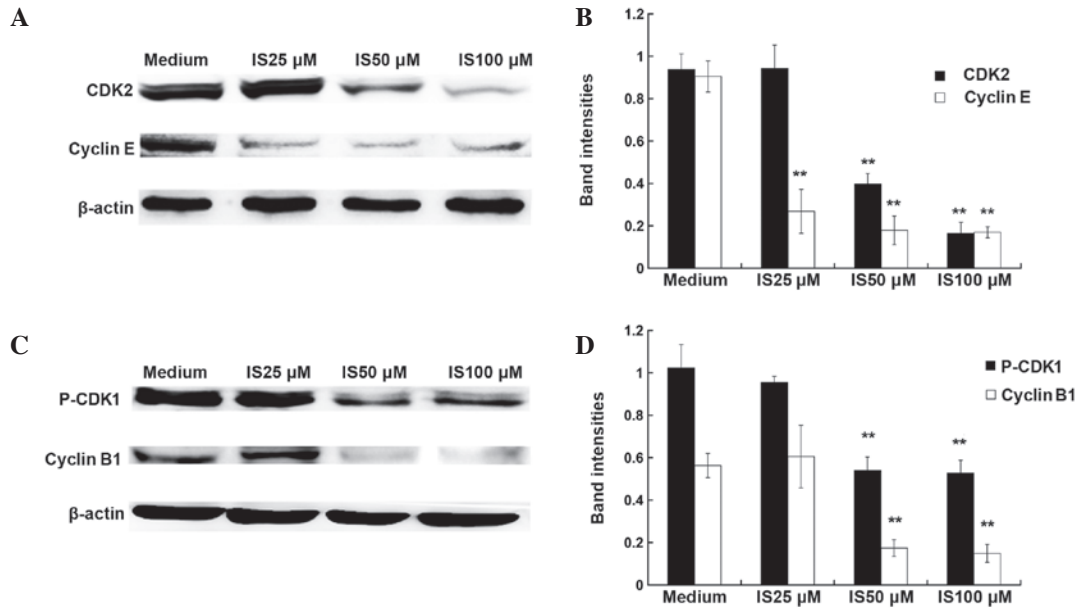


Figure 2. Icariside II (IS) inhibits the expression of cell cycle-related proteins. A375 cells were treated with different concentrations of IS (0, 25, 50 and 100 μM) for 24 h. Cell cycle-related proteins, such as CDK2, cyclin E, P-CDK1 and cyclin B1 were detected by western blot analysis. All lanes were loaded with 30 μg protein and β-actin was used as the loading control. Band intensities were quantified using UN-SCAN-IT Gel Analysis software. The optical density for target protein was shown as a proportion of β-actin optical density. \*\*P<0.01, as compared with medium control group. (A) Representative western blot images of CDK2 and cyclin E. (B) Quantification of band intensities of CDK2 and cyclin E. (C) Representative western blot images of p-CDK1 and cyclin B1. (D) Quantification of band intensities of p-CDK1 and cyclin B1.

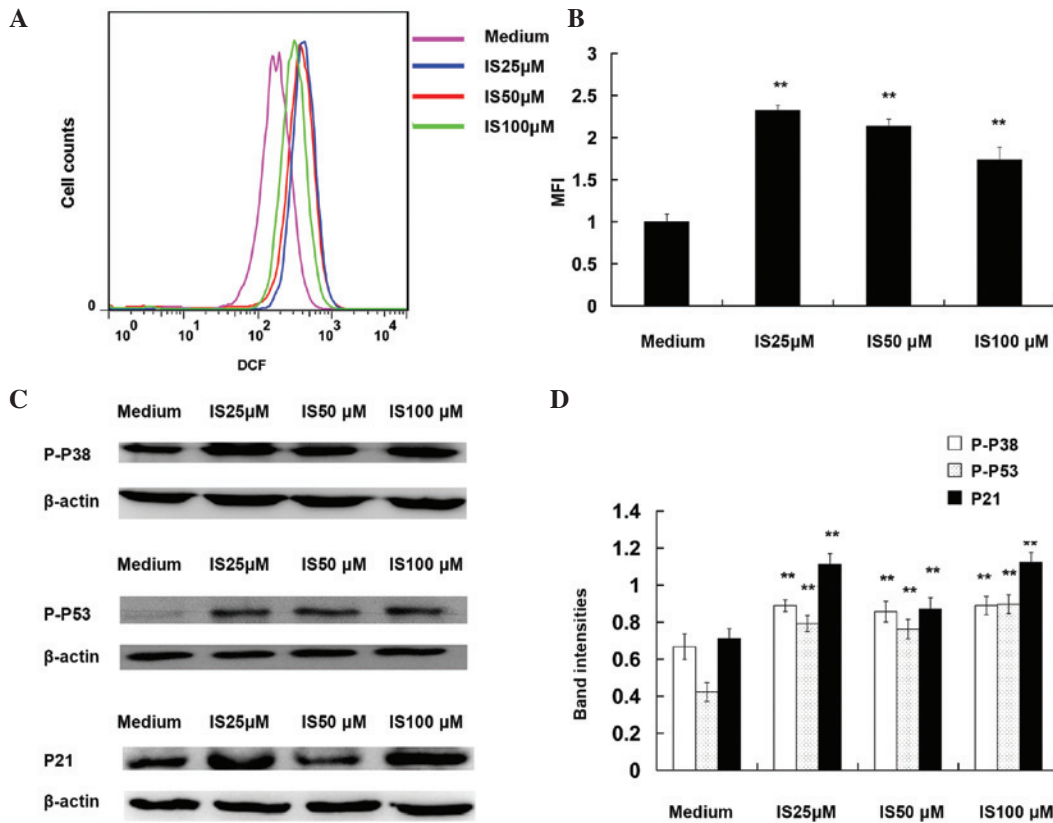


Figure 3. Icariside II (IS) induces the production of reactive oxygen species (ROS) and activates p38, p53 and p21. For the ROS assay, A375 cells were exposed to various concentrations of IS (0, 25, 50 and 100 μM) for 6 h and then were loaded with 2,7-dichlorodihydrofluorescein diacetate (10 μM). Following incubation at 37°C for 30 min, cells were washed with phosphate-buffered saline and their fluorescence measured using either flow cytometry or fluorescence microscopy. The mean fluorescence intensity (MFI) data were analyzed with FlowJo software V6.0. (A) Representative images of ROS MFI. (B) Statistical data of ROS MFI. For western blotting assays, A375 cells were treated with different concentrations of IS (0, 25, 50 and 100 μM) for 24 h. The total protein were extracted, and the levels of P-p38, P-p53 and p21 were detected by western blot analysis. β-actin was used as the loading control. (C) Representative western blot images of P-p38, P-p53 and p21. (D) Quantification of band intensities of P-p38, P-p53, and p21. Band intensities were quantified using UN-SCAN-IT Gel Analysis software. \*\*P<0.01, as compared with medium control group.

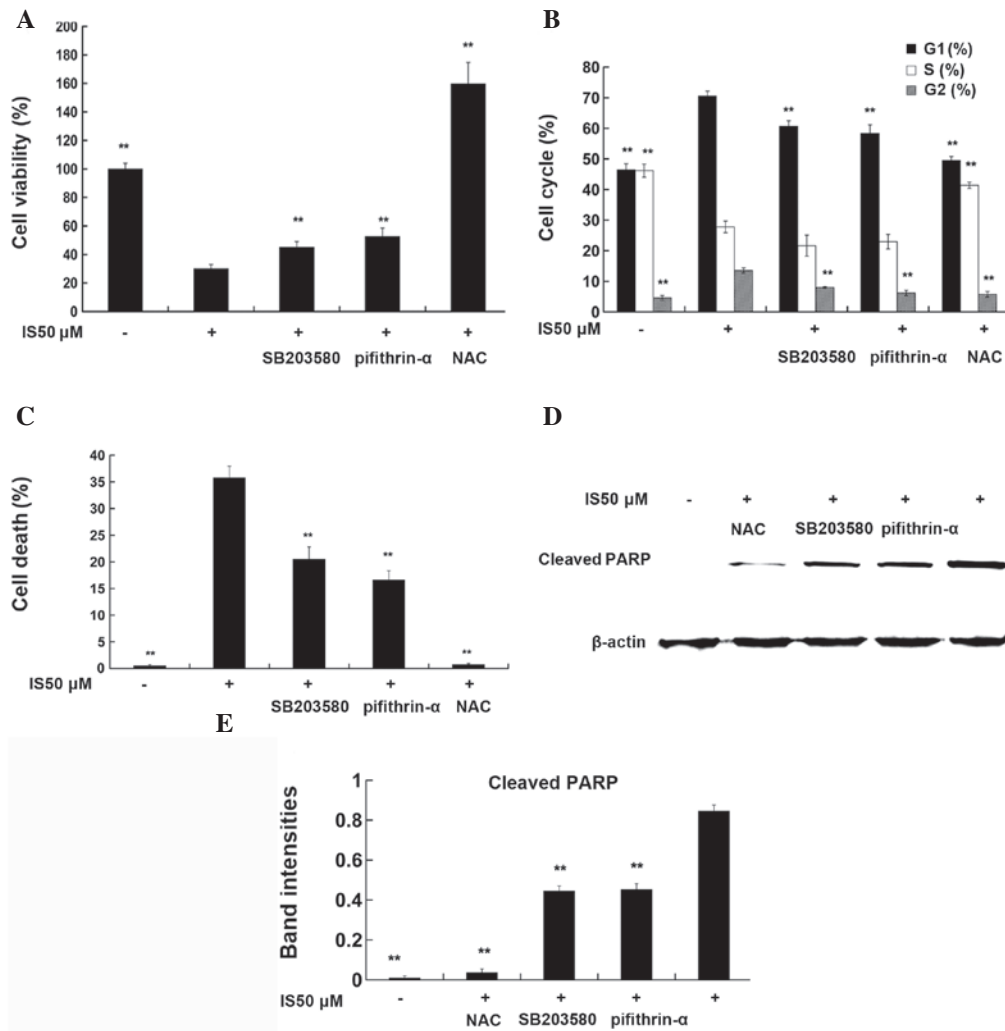


Figure 4. Icariside II (IS)-mediated reduction of cell viability, increase of cell cycle arrest, increase of cell death and PARP cleavage were reversed by NAC, SB203580 and pifithrin- $\alpha$ . The cells were pretreated with or without NAC (2 mM), SB203580 (5  $\mu$ M) or pifithrin- $\alpha$  (5  $\mu$ M) for 1 h followed by culture with 50  $\mu$ M IS for 24 h. (A) Cell viability assays. Following IS treatment for 24 h, WST-8 solutions were added for 1 h. The optical density data were detected in a plate reader at 450 nm. (B) Cell cycle assay. (C) Cell death assay. Following fixation, the cells were stained with propidium iodide and then analyzed using a FACSCalibur™ cytometer. The cell cycle and death data were analyzed using FlowJo software V6.0. (D) Representative western blot images of cleaved PARP.  $\beta$ -actin was used as the loading control. (E) Quantification of band intensities of cleaved PARP. Band intensities were quantified using UN-SCAN-IT Gel Analysis software. The optical density for target protein was shown as a proportion of  $\beta$ -actin optical density. \*\*P<0.01, as compared with 50  $\mu$ M IS treatment alone group.

that in the medium controls (P<0.01). Pretreatment with NAC (2 mM), a ROS scavenger, for 1 h completely reversed the IS-mediated reduction in cell viability (P<0.01), while pretreatment with SB203580 (5  $\mu$ M), a p38 inhibitor, or pifithrin- $\alpha$  (5  $\mu$ M), a p53 inhibitor, for 1 h partially reversed the IS-mediated reduction of cell viability (P<0.01). Cell cycle data (Fig. 4B) demonstrated that 50  $\mu$ M IS treatment induced G0/G1 phase and G2/M phase arrest compared with that in the medium controls (P<0.01), while pretreatment with NAC, SB203580 or pifithrin- $\alpha$  reversed IS-induced cell cycle arrest, respectively (P<0.01). Fig. 4C shows that treatment with IS 50  $\mu$ M for 24 h resulted in a marked increase in the levels of cell death (33.60%) compared with those in the medium control (0.26%). NAC, SB203580 or pifithrin- $\alpha$  pretreatment partly reversed the IS-mediated increase in the levels of cell death (P<0.01). Similar trends were observed in the levels of cleaved PARP, a marker of cells undergoing apoptosis (Fig. 4D and E).

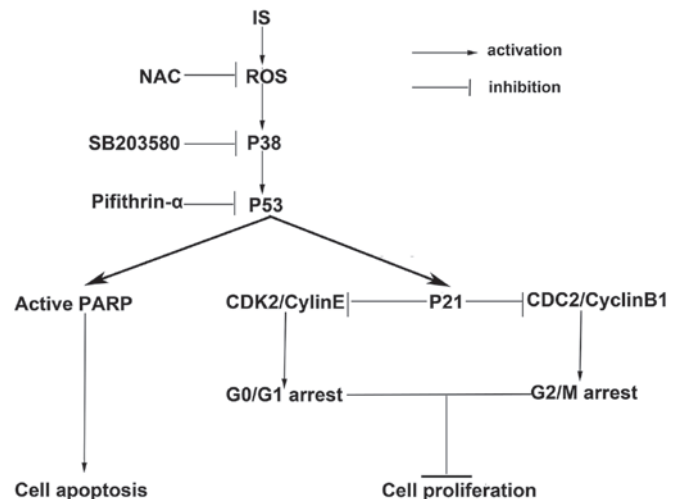


Figure 5. Schematic representation of the probable pathway involved in icaricide II (IS)-induced proliferation inhibition, cell cycle arrest and death of A375 cells.

## Discussion

Since deregulated proliferation and inhibition of apoptosis are key processes in the development of all types of tumor, they present two clear targets for therapeutic intervention in tumors (21). In the current study, the cell counting data demonstrated that IS markedly inhibited cell proliferation in A375 melanoma cells. The rate of cell proliferation is also identified through the calculation of the proportion of cells in various phases of the cell cycle, with the easiest being the S phase (22). The cell cycle data showed that IS significantly reduced the proportion of A375 melanoma cells in the S phase, which further supports the anti-proliferative effects of IS.

Uncontrolled cellular proliferation is the result of cell cycle disorganization (22). Numerous families of regulatory proteins possess key roles in the control of cell cycle progression, including the cyclins, CDKs, their substrate proteins, the CDK inhibitors and the tumor-suppressor gene products p53 and pRb (20). These families comprise the basic regulatory machinery responsible for catalyzing cell cycle transition. For example, the cyclin E-CDK2 complex has a critical role in the G1/S phase transition (23) and the cyclin B1-CDK1 complex is expressed predominantly during G2/M phase (24). Data from the present study showed that IS-induced cell cycle arrest of A375 cells predominantly occurs during the G0/G1 phase, occurring to a lesser extent during the G2/M phase. These effects were mediated by inhibition of cell cycle-related proteins, such as cyclin E, CDK2, cyclin B1 and CDK1. A previous study reported that IS could potentiate paclitaxel-induced cell death in A375 human melanoma cells (25). Paclitaxel mainly induces the cell cycle blockage at the G2/M boundary (26,27), while IS mainly induces the cell cycle blockage at the G1/S boundary. The synergistic mechanism may be attributed to different cell cycle regulation of these two compounds.

Evidence from a previous study implies that there is a positive correlation between cellular redox status and cytotoxic efficacy of anti-cancer agents (28). The present study reported that IS inhibited the cell viability and cell proliferation through the generation of ROS. These findings were further supported by the evidence that pretreatment with NAC blocked IS-mediated reduction of cell viability, increase of cell death and cell cycle arrest. Following IS treatment (6 h), the ROS levels in the 100  $\mu$ M IS treatment group were lower than those in the 50 and 25  $\mu$ M IS treatment groups. These ROS data were inconsistent with the cell viability and proliferation data. Perhaps the time elapsed for ROS production to reach a peak level following treatment with 100  $\mu$ M IS, is significantly less than that after treatment with 25 and 50  $\mu$ M.

A previous study has indicated that ROS induces the activation of the MAPK pathways and that the activation of p38 MAPK is involved in cell growth arrest (24). p38 MAPK activation leads to accumulation of p53 by directly phosphorylating it at selected amino acid residues (29). p53 protein is an important cell cycle check-point regulator at the G1/S and G2/M check points (30,31). p53-dependent cell cycle arrest is mainly mediated by transcriptional activation of p21 (24). In this study, it was revealed that IS treatment induced massive ROS accumulation in A375 cells, and activated a series of important related proteins, including p38, p53 and p21. These results were further supported by the evidence

that pretreatment with SB203580 or pifithrin- $\alpha$  significantly blocked IS-mediated reduction of cell viability, increase of cell death and cell cycle arrest. Therefore, it was determined that the ROS-mediated p38-p53 signaling pathway was involved in IS-induced reduction of cell viability and cell proliferation, increase of cell death and cell cycle arrest (Fig. 5).

In the present study, SB203580 and pifithrin- $\alpha$  pretreatment failed to completely reverse IS-induced cell death and cell cycle arrest. These findings suggested that other important mechanisms may be involved in IS-mediated cytotoxic effects. A previous study demonstrated that IS sensitized U937 acute myeloid leukemia cells to apoptosis via activating JAK2-STAT3 signaling (20). Further studies are necessary to investigate the association between IS-mediated activation of the ROS-p38-p53 signaling pathway and inactivation of the JAK2-STAT3 signaling pathway in human melanoma cells.

In conclusion, the present study reports that IS inhibits cell proliferation and induces cell cycle arrest. Additionally, it confirms that these effects are mediated at least in part by activation of the ROS-p38-p53 signaling pathway. These findings suggest that IS may be a potential chemotherapeutic agent in treatment of melanoma in the future.

## Acknowledgements

This study was funded by a grant from the National Natural Science Foundation of China (81102541).

## References

- Rigel DS, Russak J and Friedman R: The evolution of melanoma diagnosis: 25 years beyond the ABCDs. *CA Cancer J Clin* 60: 301-316, 2010.
- Balch CM, Gershenwald JE, Soong SJ, *et al*: Final version of 2009 AJCC melanoma staging and classification. *J Clin Oncol* 27: 6199-6206, 2009.
- Soengas MS and Lowe SW: Apoptosis and melanoma chemoresistance. *Oncogene* 22: 3138-3151, 2003.
- Serrone L, Zeuli M, Segal FM and Cognetti F: Dacarbazine-based chemotherapy for metastatic melanoma: thirty-year experience overview. *J Exp Clin Cancer Res* 19: 21-34, 2000.
- Tsao H, Atkins MB and Sober AJ: Management of cutaneous melanoma. *N Engl J Med* 351: 998-1012, 2004.
- Panka DJ, Atkins MB and Mier JW: Targeting the mitogen-activated protein kinase pathway in the treatment of malignant melanoma. *Clin Cancer Res* 12: 2371s-2375s, 2006.
- Boutros T, Chevret E and Metrakos P: Mitogen-activated protein (MAP) kinase/MAP kinase phosphatase regulation: roles in cell growth, death, and cancer. *Pharmacol Rev* 60: 261-310, 2008.
- Dolado I, Swat A, Ajenjo N, De Vita G, Cuadrado A and Nebreda AR: p38alpha MAP kinase as a sensor of reactive oxygen species in tumorigenesis. *Cancer Cell* 11: 191-205, 2007.
- Assefa Z, Vantieghem A, Garmyn M, *et al*: p38 mitogen-activated protein kinase regulates a novel, caspase-independent pathway for the mitochondrial cytochrome c release in ultraviolet B radiation-induced apoptosis. *J Biol Chem* 275: 21416-21421, 2000.
- Bulavin DV, Demidov ON, Saito S, *et al*: Amplification of PPM1D in human tumors abrogates p53 tumor-suppressor activity. *Nat Genet* 31: 210-215, 2002.
- Vogelstein B, Lane D and Levine AJ: Surfing the p53 network. *Nature* 408: 307-310, 2000.
- Xiao D, Powolny AA, Moura MB, *et al*: Phenethyl isothiocyanate inhibits oxidative phosphorylation to trigger reactive oxygen species-mediated death of human prostate cancer cells. *J Biol Chem* 285: 26558-26569, 2010.
- Xiao D, Powolny AA and Singh SV: Benzyl isothiocyanate targets mitochondrial respiratory chain to trigger reactive oxygen species-dependent apoptosis in human breast cancer cells. *J Biol Chem* 283: 30151-30163, 2008.

14. Lee KS, Lee HJ, Ahn KS, *et al*: Cyclooxygenase-2/prostaglandin E2 pathway mediates icariside II induced apoptosis in human PC-3 prostate cancer cells. *Cancer Lett* 280: 93-100, 2009.
15. Kim SH, Ahn KS, Jeong SJ, *et al*: Janus activated kinase 2/signal transducer and activator of transcription 3 pathway mediates icariside II-induced apoptosis in U266 multiple myeloma cells. *Eur J Pharmacol* 654: 10-16, 2011.
16. Kang SH, Jeong SJ, Kim SH, *et al*: Icariside II induces apoptosis in U937 acute myeloid leukemia cells: role of inactivation of STAT3-related signaling. *PloS one* 7: e28706, 2012.
17. Xia Q, Xu D, Huang Z, Liu J, Wang X and Liu S: Preparation of icariside II from icariin by enzymatic hydrolysis method. *Fitoterapia* 81: 437-442, 2010.
18. Röhner E, Kolar P, Seeger JB, *et al*: Toxicity of antiseptics against chondrocytes: what is best for the cartilage in septic joint surgery? *Int Orthop* 35: 1719-1723, 2011.
19. Röhner E, Matziolis G, Perka C, *et al*: Inflammatory synovial fluid microenvironment drives primary human chondrocytes to actively take part in inflammatory joint diseases. *Immunol Res* 52: 169-175, 2012.
20. Gali-Muhtasib H and Bakkar N: Modulating cell cycle: current applications and prospects for future drug development. *Curr Cancer Drug Targets* 2: 309-336, 2002.
21. Evan GI and Vousden KH: Proliferation, cell cycle and apoptosis in cancer. *Nature* 411: 342-348, 2001.
22. Golias CH, Charalabopoulos A and Charalabopoulos K: Cell proliferation and cell cycle control: a mini review. *Int J Clin Pract* 58: 1134-1141, 2004.
23. Ma T, Van Tine BA, Wei Y, *et al*: Cell cycle-regulated phosphorylation of p220(NPAT) by cyclin E/Cdk2 in Cajal bodies promotes histone gene transcription. *Genes Dev* 14: 2298-2313, 2000.
24. Kawamoto H, Koizumi H and Uchikoshi T: Expression of the G2-M checkpoint regulators cyclin B1 and cdc2 in nonmalignant and malignant human breast lesions: immunocytochemical and quantitative image analyses. *Am J Pathol* 150: 15-23, 1997.
25. Wu J, Guan M, Wong PF, Yu H, Dong J and Xu J: Icariside II potentiates paclitaxel-induced apoptosis in human melanoma A375 cells by inhibiting TLR4 signaling pathway. *Food Chem Toxicol* 50: 3019-3024, 2012.
26. Schiff PB and Horwitz SB: Taxol stabilizes microtubules in mouse fibroblast cells. *Proc Natl Acad Sci USA* 77: 1561-1565, 1980.
27. Crossin KL and Carney DH: Microtubule stabilization by taxol inhibits initiation of DNA synthesis by thrombin and by epidermal growth factor. *Cell* 27: 341-350, 1981.
28. Engel RH and Evens AM: Oxidative stress and apoptosis: a new treatment paradigm in cancer. *Front Biosci* 11: 300-312, 2006.
29. Bulavin DV, Saito S, Hollander MC, *et al*: Phosphorylation of human p53 by p38 kinase coordinates N-terminal phosphorylation and apoptosis in response to UV radiation. *EMBO J* 18: 6845-6854, 1999.
30. She QB, Chen N and Dong Z: ERKs and p38 kinase phosphorylate p53 protein at serine 15 in response to UV radiation. *J Biol Chem* 275: 20444-20449, 2000.
31. Kastan MB, Canman CE and Leonard CJ: P53, cell cycle control and apoptosis: implications for cancer. *Cancer Metastasis Rev* 14: 3-15, 1995.